Journal of Molecular Structure: THEOCHEM 941 (2010) 144–149

Contents lists available at ScienceDirect

Journal of Molecular Structure: THEOCHEM

journal homepage: www.elsevier.com/locate/theochem

Ab initio investigation of hydrogenation of $(BN)_{16}$: A comparison with that of $(BN)_{12}$

Xiao-Ying Cui [a,b], Bin-Sheng Yang [a], Hai-Shun Wu [b,*]

[a] Institute of Molecular Science, Shanxi University, Taiyuan 030006, China
[b] School of Chemistry and Material Science, Shanxi Normal University, Linfen 041004, China

ARTICLE INFO

Article history:
Received 10 August 2009
Received in revised form 10 November 2009
Accepted 12 November 2009
Available online 6 December 2009

Keywords:
Density functional theory
$B_{16}N_{16}H_n$ and $B_{12}N_{12}H_n$
Structure
Hydrogen storage
Average binding energy

ABSTRACT

The hydrogenation of $B_{16}N_{16}$ cage has been studied using ab initio molecular orbital theory with B3LYP/6-31G(d) method. The structure characters of the most stable $B_{16}N_{16}H_n$ (n = 2–32) isomers are discussed in detail. The results show that the average binding energies of hydrogenated $B_{16}N_{16}$ cage are smaller than that of $B_{12}N_{12}$ cage especially in high hydrogen coverage. The smaller angle distortion and shorter average B–N bond length of $B_{16}N_{16}$ are the main reason for the smaller average binding energy per H_2 of $B_{16}N_{16}H_n$ comparing with $B_{12}N_{12}H_n$. Gibbs free energy calculation shows the reaction of $B_{16}N_{16} + 16H_2 \rightarrow B_{16}N_{16}H_{32}$ will reverse at about 110 K, which is lower than the reversing temperature 320 K for the reaction of $B_{12}N_{12} + 12H_2 \rightarrow B_{12}N_{12}H_{24}$.

1. Introduction

Hydrogen is attractive as a fuel because its use creates neither air pollution nor greenhouse-gas emissions [1–3]. The use of hydrogen requires an effective, safe, and stable storage medium. However, how to store hydrogen easily and cheaply is still one of the key challenges in developing hydrogen economy [4,5]. Considerable attentions have been focused on porous materials such as metal–organic frameworks (MOF's), clathrates, carbon nanotubes, fullerenes and organic hosts as possible materials for hydrogen storage [6–11]. Non-carbon nanosystem comprised of light elements such as boron and nitrogen atoms also have been noticed [12,13].

Boron nitride nanostructures have a wide range of attractive properties, such as high-temperature stability, a low dielectric constant, large thermal conductivity, and oxidation resistance, leading to a number of potential applications as a structural or electronic material [14–16]. The heteropolar nature in the BN nanostructures offers higher binding energy for hydrogen storage compared to the carbon based materials [17]. It has been found experimentally that at 10 MPa the BN nanotubes can store as much as 2.6 wt.% of hydrogen and that collapsed BN nanotubes exhibit an even higher storage capacity (4.2 wt.%) [18,19].

Hydrogen storage capacity and mechanism of BN nanotubes and sheets have been well investigated [20–29]. The BN cages also have received much attention since their potential advantages in hydrogen storage due to their large surface area [30–36]. When only chemical adsorption being considered. One hundred percent coverage can achieve 7.7 wt.% of hydrogen storage. It was found that $B_{12}N_{12}$, $B_{16}N_{16}$ and $B_{28}N_{28}$ stand out as "magic" BN-fullerenes [37–39]. The DFT investigation of hydrogenation of the small $B_{12}N_{12}$ shows that $B_{12}N_{12}$ may be a proper candidate material for hydrogen storage [40]. Considering that it is difficult to obtain unique sized B_nN_n cage, it is necessary to explore the hydrogen storage ability of larger B_nN_n cage and to conclude how the size of B_nN_n cage affect its hydrogen storage ability. In this work, the chemisorption behavior of hydrogen on $B_{16}N_{16}$ cage with different coverage is investigated based on DFT calculations. Also a comparison with the results of $B_{12}N_{12}$ cage has be done, which might be a useful guidance to the experimental studies of hydrogenation of BN nanomaterials.

2. Computational details

All computations were performed at B3LYP/6-31G(d) level of density functional theory with the Gaussian 03 program packages [41]. The B3LYP/6-31G(d) method can give reasonable results for BN cages [42] and their derivative [40,43]. The convergence criteria for structure optimizations and energy calculations in this work were set to default values in Gaussian 03 package. Namely, the energy convergence criteria in both SCF and electron density calculations is 1.0×10^{-6} hartree. In geometry optimizations, the cutoff values for force and displacement are 0.00045 hartree/bohr and 0.0018 bohr, respectively. All isomers considered in this work have been fully optimized without symmetry constrains. The frequency calculations for these isomers were performed at B3LYP/6-31g(d)

* Corresponding author. Tel.: +86 357 2052468; fax: +86 357 2051375.
E-mail address: wuhs@mail.sxtu.edu.cn (H.-S. Wu).

0166-1280/$ - see front matter © 2009 Elsevier B.V. All rights reserved.
doi:10.1016/j.theochem.2009.11.023

level to characterize the nature of the optimized structures and get zero point energy (ZPE) corrections. All of the most stable isomers reported are minima in their potential energy surfaces without imaginary frequencies. The average binding energy (ABE) per H_2 molecule is defined as $2/n\{E(B_{16}N_{16}) + n/2E\ (H_2) - E(B_{16}N_{16}H_n)\}$ as in Ref. [40], where $E(X)$ means the total energy with ZPE correction of species and n is the number of hydrogen atoms. In Tables 1 and 2, we list both the ABEs with and without ZPE correction for considered hydrogenated $B_{16}N_{16}$ cages. The ABE without ZPE correction is only used for comparing with the literature result for hydrogenated $B_{12}N_{12}$ cages [40].

3. Results and discussion

3.1. The structural character and average binding energy of one hydrogen molecule adsorption

There are three unique B–N bond types among the 48 B–N bonds in the most sable $B_{16}N_{16}$ cage [44]; one is shared by a four- and a six-membered ring (R_{46}), and the other two by two six-membered rings (R_{66}). Similar to $B_{12}N_{12}$ cluster, R_{46} (1.473 Å) is slightly longer than R_{66} (1.458 and 1.456 Å) and they are all shorter than the single bond in H_3B–NH_3 (1.668 Å), but longer than the double bond in $H_2B{=}NH_2$ (1.393 Å) at B3LYP/6-31G(d). The average B–N bond length of $B_{16}N_{16}$ (1.465 Å) is smaller than that of $B_{12}N_{12}$ (1.471 Å) [45]. The difference between R_{46} and R_{66} of $B_{16}N_{16}$ (0.015 and 0.017 Å) is smaller than that of $B_{12}N_{12}$ (0.047 Å), which indicates that π electrons in $B_{16}N_{16}$ cage are more delocalized than those in $B_{12}N_{12}$.

For the adsorption of one H_2 molecule on $B_{16}N_{16}$ cage, we examined the various modes of adsorption which shown in Fig. 1.

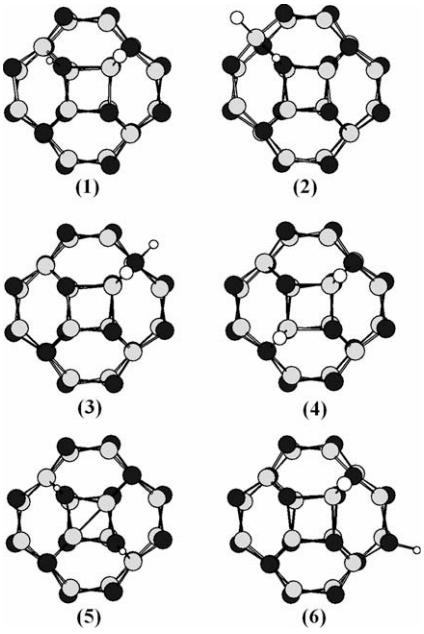

Fig. 1. Optimized geometries of the $B_{16}N_{16}H_2$ clusters with B3LYP/6-31G(d) model chemistry. Black, gray and white balls stand for N, B and H, respectively. (**1**) 1,2 addition (R_{46}); (**2**) 1,2 addition (R_{661}); (**3**) 1,2 addition (R_{662}); (**4**) 1,3 addition (BB); (**5**) 1,3 addition (NN); (**6**) 1,4 addition.

Table 1
ABE (in kcal/mol) of $B_{16}N_{16}H_2$ with and without ZPE correction at B3LYP/6-31G(d) level and the results of $B_{12}N_{12}H_2$ without ZPE correction from literature [40].

Isomer	Adsorption mode	$B_{16}N_{16}H_2$	$B_{16}N_{16}H_2$ (without ZPE correction)	$B_{12}N_{12}H_2$
1	1,2 addition (R_{46})	2.63	8.72	9.38
2	1,2 addition (R_{661})	−10.31	−4.14	8.64
3	1,2 addition (R_{662})	−16.47	−10.83	–
4	1,3 addition (BB)	−97.97	−98.19	−64.17
5	1,3 addition (NN)	−78.31	−72.79	–
6	1,4 addition	−14.42	−8.62	−6.50

Table 2
ABE (in kcal/mol) of $B_{16}N_{16}H_n$ (n = 4, 6, 8, 10, 12, 14, 16, 20, 24, 28 and 32) with and without ZPE correction at B3LYP/6-31G(d) level.

Isomer	Formula	Symmetry	ABE	ABE (without ZPE correction)
7	$B_{16}N_{16}H_4$	C_{2v}	7.96	14.77
8	$B_{16}N_{16}H_6$	C_1	6.85	13.58
9	$B_{16}N_{16}H_8$	D_{2d}	8.10	15.05
10	$B_{16}N_{16}H_{10}$	C_1	5.57	12.33
11	$B_{16}N_{16}H_{12}$	C_2	5.24	12.07
12	$B_{16}N_{16}H_{14}$	C_1	6.33	13.09
13		C_1	4.21	10.97
14	$B_{16}N_{16}H_{16}$	C_{2v}	6.46	13.31
15		D_{2d}	3.88	10.65
16		C_2	3.63	10.30
17	$B_{16}N_{16}H_{20}$	C_{2v}	4.98	12.20
18	$B_{16}N_{16}H_{24}$	C_1	3.97	11.31
19	$B_{16}N_{16}H_{28}$	C_s	3.20	10.62
20	$B_{16}N_{16}H_{32}$	T_d	1.95	9.60

Isomer **1** represents the R_{46} bond adsorption of the 1, 2 addition, while isomer **2** and **3** represent two different R_{66} bond adsorptions of the 1, 2 addition. Similar to $B_{12}N_{12}H_2$ [40], we found that the isomer **1** with R_{46} bond adsorption of the 1, 2 addition is the most favorable. The ABEs in Table 1 show that the R_{46} bond adsorption of 1, 2 addition (2.63 kcal/mol) is more favorable than the R_{66} bond adsorption (−10.31 and −16.47 kcal/mol). The R_{46} bond adsorption is slightly exothermic while both R_{66} adsorptions are endothermic. Isomer **4** and **5** represent two different modes of the 1, 3 addition. In isomer **4** two hydrogen atoms bind with two boron atoms while in **5** with two nitrogen atoms. Isomer **4** can only be obtained with symmetry constraint, otherwise it will be optimized to other structures. It is not a minimum on the potential energy surface since having an imaginary frequency. The most stable structure of 1, 4 addition is shown as isomer **6**.

As shown in Table 1, it is obvious that ABEs of the 1, 3 addition (isomer **4**, **5**) and 1, 4 addition (isomer **6**) are all smaller than that of R_{46} bond adsorption (isomer **1**) and the ABEs of all adsorption modes for $B_{16}N_{16}$ are smaller than that of $B_{12}N_{12}$. It's worth noting that the most favorable R_{46} bond adsorption for $B_{16}N_{16}$ and $B_{12}N_{12}$ have similar ABE (8.72 and 9.38 kcal/mol without ZPE correction), while for R_{66} bond adsorptions, $B_{16}N_{16}$ has negative ABEs (−4.14 and −10.83 kcal/mol without ZPE correction), dramatically different from the positive ABE of $B_{12}N_{12}$ (8.62 kcal/mol without ZPE correction).

As we mentioned above, both R_{46} and R_{66} bonds of $B_{16}N_{16}$, dominated by stronger delocalized π electrons, are shorter than that of $B_{12}N_{12}$. The elongated bonds in $B_{12}N_{12}$ could induce high surface potential energy that increases the surface reactivity [46]. The destruction of delocalized π orbital in $B_{16}N_{16}$ by hydrogenation would imply more energy loss than in $B_{12}N_{12}$. Additional, the local curvature and topology of the cage surface have important impact on the binding energy. An approximate linear relation between adsorption energy and pyramidalization angle has been found for various CNTs and BNNTs with different diameters. Correspondingly, the reactivity of these CNT and BNNTs decreases with the increase of tube diameter due to the reduction of surface curvature

[47,48]. The π-orbital axis vectors (POAV) calculated by Zhu and his coworkers show that the surface of $B_{12}N_{12}$ is more curved than $B_{16}N_{16}$ [49], and correspondingly $B_{12}N_{12}$ undergoes more strain than $B_{16}N_{16}$.

The boron and nitrogen atoms of $B_{12}N_{12}$ and $B_{16}N_{16}$ cages are all sp^2 hybridization. They are converted from sp^2 to sp^3 hybridization with the H adsorbed on them [50]. Detailed inspection of the structures of $B_{12}N_{12}$ and $B_{16}N_{16}$ shows that the bond angles around boron or nitrogen vertices are all deviated from the perfect sp^2 angle 120°. To estimate the strain energy caused by this deviation, we can define the angle distortion (*AD*) of a boron vertex and a nitrogen vertex of a B–N bond [51–53] by Eq. (1), where *A* is the BNB angle around nitrogen vertex and *B* is NBN angle around boron vertex. The *AD* of R_{46} in $B_{12}N_{12}$ (45.4°) is greater than that of R_{46} in $B_{16}N_{16}$ (41.7°), which indicates that R_{46} of $B_{12}N_{12}$ is more easily to be broken than that of $B_{16}N_{16}$. So it is not surprised why $B_{12}N_{12}H_2$ has slightly greater ABE than $B_{16}N_{16}H_2$. The *AD* of R_{66} (28.1° and 28.4°) in $B_{16}N_{16}$ is much smaller than that of R_{46} (41.7°), which explains why the ABE of isomer **2** and **3** is much smaller than that of isomer **1**.

$$AD_{B-N} = \left(\sum |120^{\circ} - A| + \sum |120^{\circ} - B|\right)/2 \quad (1)$$

3.2. The structural character and average binding energy of increasing hydrogen coverage

To clarify the character of more hydrogen adsorption process in detail, various isomers of the given hydrogen-covered $B_{16}N_{16}H_n$ (n = 4, 6, 8, 10, 12, 14, 16, 20, 24, 28 and 32) are examined. The structures of the most favorable and some less favorable isomers are shown in Figs. 2 and 3, and their ABEs are summarized in Table 2.

In Fig. 2, it is obvious that for all most stable structures, hydrogen additions occur on R_{46} bonds. So it can be concluded that when $n \leqslant 16$, H atoms prefer to adsorb on the R_{46} bonds in pairs form, which confirms well the result of previous section.

More detailed inspection of the isomer geometries in Fig. 2 shows that H atoms favor the four-member rings on $B_{16}N_{16}$. For example, in the most favorable isomer of $B_{16}N_{16}H_4$ (**7**) two H_2 molecules adsorb on a four-membered ring; in the most favorable isomer of $B_{16}N_{16}H_8$ (**9**) four H_2 molecules adsorb on two opposite four-membered rings; in the most favorable isomer of $B_{16}N_{16}H_{12}$ (**11**) six H_2 molecules adsorb on three tandem four-membered rings; and in the second most favorable isomer of $B_{16}N_{16}H_{16}$ (**15**) eight H_2 molecules adsorb on four tandem four-membered rings. In the most favorable isomer of $B_{16}N_{16}H_6$ (**8**), $B_{16}N_{16}H_{10}$ (**10**) and the second most favorable isomer of $B_{16}N_{16}H_{14}$ (**13**), the additional one H_2 molecule prefer to adsorb on the adjacent four-membered ring. The structure charter of these adsorbed isomers also is found in hydrogenated BN (0 0 0 1) surface recently [54].

We found some interesting exceptions that the structures of the most favorable isomers of $B_{16}N_{16}H_{14}$ (**12**) and $B_{16}N_{16}H_{16}$ (**14**) are different from that of other $B_{16}N_{16}H_n$ (n < 14). The ABE of **12** (6.33 kcal/mol) for $B_{16}N_{16}H_{14}$ is greater than the corresponding isomer **13** (4.21 kcal/mol), and **14** (6.46 kcal/mol) for $B_{16}N_{16}H_{16}$ are more stable than the corresponding isomer **15** (3.88 kcal/mol). **13** and **15** are based on the most stable structure for $B_{16}N_{16}H_n$ with n < 14. **12** and **14** have flat structure in which all H atoms adsorb on the R_{46} bonds locating at circumference of the flat cage and the two opposite six-membered rings locating at the centre keep uncovered. Furthermore, some broken B–N bonds occur on the hydrogenated four-membered rings. The distance of B and N atom on the broken B–N bond is about 2.80 Å.

Fig. 4 shows some selected orbital of $B_{16}N_{16}H_{16}$ (**14**). It is evident that the atoms on the non-hydrogenated six-membered rings form a typical conjugative π orbital as in benzene. So, the non-hydrogenated six-membered rings should be the main factor to stabilize the **12** and **14**. Moreover, we maybe expect that the non-hydrogenated six-membered ring is also favored when increasing hydrogen coverage. This point of view is confirmed by the $B_{16}N_{16}H_{20}$ (**17**) and $B_{16}N_{16}H_{24}$ (**18**) as shown in Fig. 3.

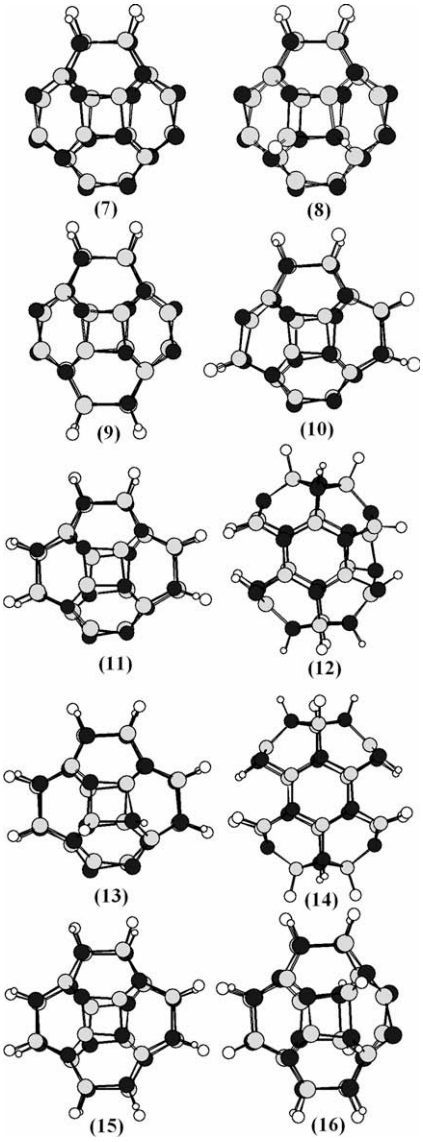

Fig. 2. Optimized geometries of the hydrogenated $B_{16}N_{16}$ clusters with B3LYP/6-31G(d) model chemistry. Black, gray and white balls stand for N, B and H, respectively. (**7**) $2H_2$-C_{2v}; (**8**) $3H_2$-C_1; (**9**) $4H_2$-D_{2d}; (**10**) $5H_2$-C_1; (**11**) $6H_2$-C_2; (**12**) $7H_2$-C_1; (**13**) $7H_2$-C_1; (**14**) $8H_2$-C_{2v}; (**15**) $8H_2$-D_{2d}; (**16**) $8H_2$-C_2.

For increasing hydrogen coverage, we confined our consideration to $B_{16}N_{16}H_n$ (n = 20, 24, 28 and 32). The most favorable isomer of $B_{16}N_{16}H_{20}$ (**17**) is also a flat structure with two planar six-membered rings retaining non-hydrogenated; the most favorable isomer of $B_{16}N_{16}H_{24}$ (**18**) can be seen a structure originated from **17** by adding two H_2 molecules on one uncovered six-membered ring, in which a planar six-membered ring and a R_{66} bond keep non-hydrogenated. The most favorable isomer of $B_{16}N_{16}H_{28}$ (**19**) is derived from **18** by adding another two H_2 molecules on the uncovered six-membered ring and keeping two R_{66} bonds non-hydrogenated. The structure of $B_{16}N_{16}H_{32}$ (**20**), i.e. 100% coverage, like $B_{16}N_{16}$, keeps T_d symmetry.

The ABE of $B_{16}N_{16}H_n$ as a function of the number of the adsorbed H atoms is presented in Fig. 5. The gravimetry hydrogen

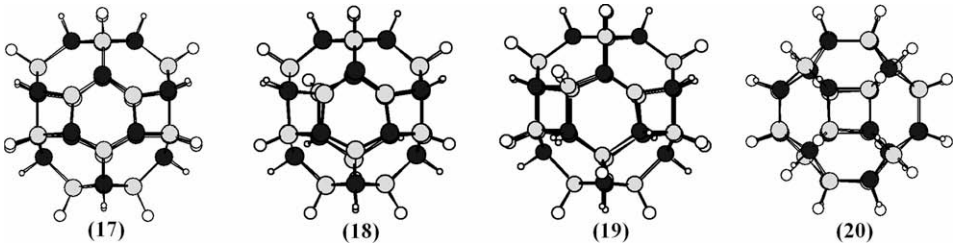

Fig. 3. Optimized geometries with B3LYP/6-31G(d) model chemistry of the hydrogenated $B_{16}N_{16}$ clusters. Black, gray and white balls stand for N, B and H, respectively. (**17**) $10H_2$-C_{2v}; (**18**) $12H_2$-C_1; (**19**) $14H_2$-C_s; (**20**) $16H_2$-T_d.

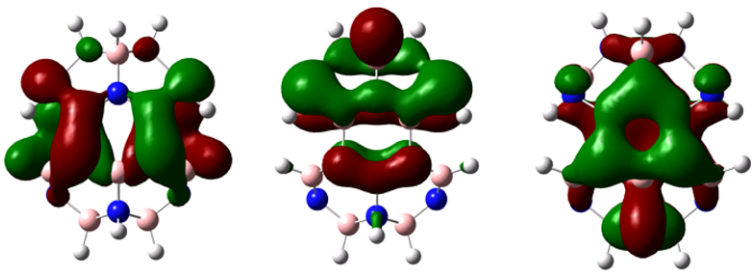

Fig. 4. The molecule orbital (MO) profiles of $B_{16}N_{16}H_{16}$ (**14**) in Fig. 2.

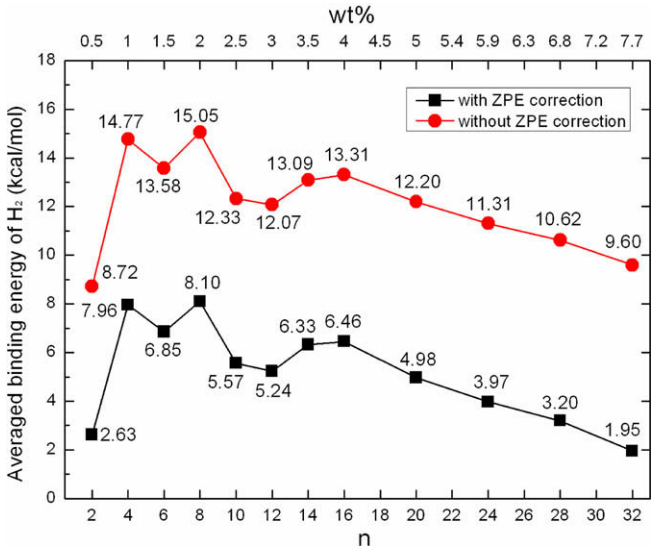

Fig. 5. ABE and hydrogen storage capacity of the $B_{16}N_{16}H_n$ (n = 2, 4, 6, 8, 10, 12, 14, 16, 20, 24, 28 and 32) at B3LYP/6-31G(d) level.

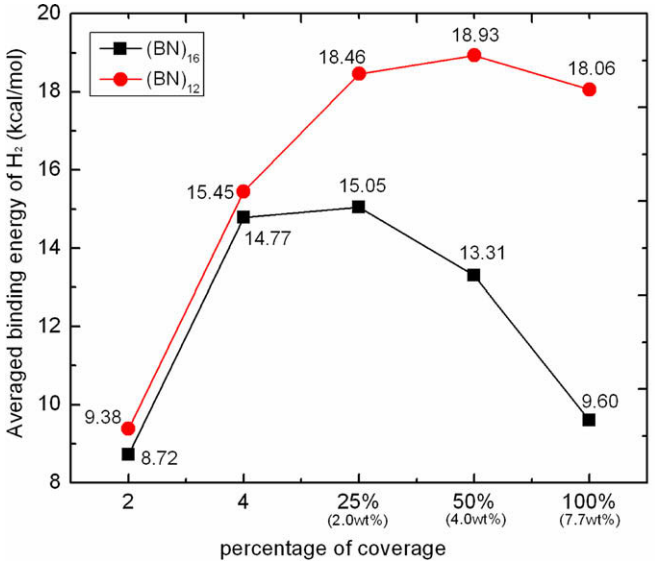

Fig. 6. ABE without ZPE correction of the $B_{16}N_{16}H_n$ and $B_{12}N_{12}H_n$ with different coverage degree at B3LYP/6-31G(d) level, where 2 and 4 represent the number of H atoms of low coverage. The data of $B_{12}N_{12}H_n$ is from literature [40].

storage expressed in wt.% of $B_{16}N_{16}H_n$ is also given in Fig. 5. As shown in Table 2 and Fig. 5, it is obvious that all these hydrogenated isomers of $B_{16}N_{16}$ have exothermic ABE, with the largest ABE 8.10 kcal/mol of $B_{16}N_{16}H_8$. When $n \geqslant 16$, the ABE of $B_{16}N_{16}H_n$ decrease gradually and seem to have a linear relationship with the number of H atoms.

To compare with hydrogenated $B_{12}N_{12}$, we present the ABEs of hydrogenated $B_{12}N_{12}H_n$ and $B_{16}N_{16}H_n$ without ZPE correction as a function of hydrogen coverage with low, 25%, 50%, 100% in Fig. 6, where low coverage represents conditions when $n = 2$ and $n = 4$. As in Fig. 5, the gravimetry hydrogen storage ratio in wt.% is also given. The ABEs of both $B_{12}N_{12}H_n$ and $B_{16}N_{16}H_n$ increase in low hydrogen coverage and achieve a peak, and then decrease with large coverage. It is obvious that the ABEs of $B_{16}N_{16}H_n$ are smaller than that of $B_{12}N_{12}H_n$ especially in high-coverage condition, i.e. the ABEs of $B_{16}N_{16}H_n$ descend more quickly than that of $B_{12}N_{12}H_n$ when hydrogen coverage becoming greater.

It is interesting to compare the stability of $B_{12}N_{12}H_{24}$ and $B_{16}N_{16}H_{32}$ based on the energy of per HBNH unit. $B_{12}N_{12}H_{24}$ is more stable than $B_{16}N_{16}H_{32}$ by 2.0 kcal/mol. In respect that $B_{16}N_{16}$ is more stable than $B_{12}N_{12}$, it is not surprising that the ABE of $B_{12}N_{12}H_{24}$ is much greater than that of $B_{16}N_{16}H_{32}$. The relative stability of $B_{12}N_{12}H_{24}$ and $B_{16}N_{16}H_{32}$ is also can be understood based on their angle distortions. In $B_{12}N_{12}H_{24}$ and $B_{16}N_{16}H_{32}$, both boron and nitrogen atoms have sp^3 hybridization. We define the angle distortion (AD) of every boron or nitrogen vertex in Eq. (2), where C is BNB and HNB, or NBN and HBN angles around nitrogen or boron vertex, and the reference angle 109.5° is perfect bond angle for sp^3 hybridization. The calculated average

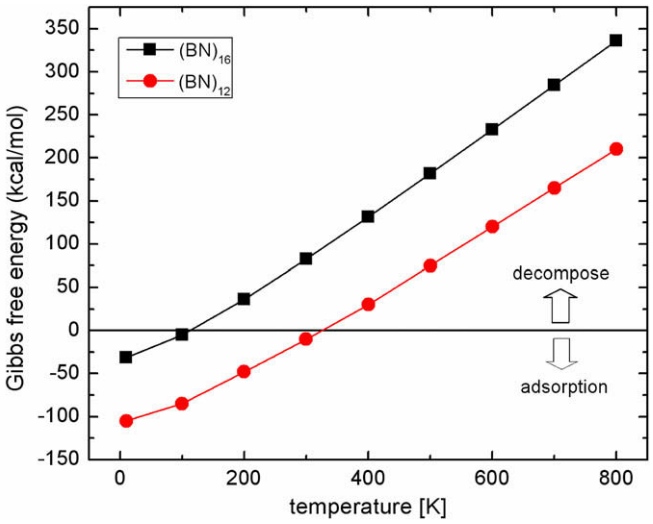

Fig. 7. Gibbs energy of the reactions of $B_{16}N_{16} + 16H_2 \rightarrow B_{16}N_{16}H_{32}$ and $B_{12}N_{12} + 12H_2 \rightarrow B_{12}N_{12}H_{24}$ with different temperature at B3LYP/6-31G(d) level. The data of the latter is from literature [40].

angle distortion of $B_{12}N_{12}H_{24}$ is 46.4°, which is smaller than 48.4° of $B_{16}N_{16}H_{32}$. The larger average angle distortion of $B_{16}N_{16}H_{32}$ indicates it is more strained than $B_{12}N_{12}H_{24}$.

$$AD_{\text{vertex}} = \sum |109.5^{\circ} - C| \quad (2)$$

3.3. Thermodynamic stability of the $B_{16}N_{16}H_{32}$ molecule

We have calculated the Gibbs free energy change of $B_{16}N_{16}$ (T_d symmetry) + $16H_2 \rightarrow B_{16}N_{16}H_{32}$ (T_d symmetry) starting at 10 K and in the range 100–800 K at increments of 100 K to compare with the reaction of $B_{12}N_{12}$ (T_h symmetry) + $12H_2 \rightarrow B_{12}N_{12}H_{24}$ (T_h symmetry) in the same temperature range. As shown in Fig. 7. It is found that the change tendency of Gibbs-free-energy of them is consistent and two reactions are all spontaneous process at low temperature. For $B_{12}N_{12}$, it becomes reverse above 320 K, while for $B_{16}N_{16}$, the reaction would be reverse above about 110 K. This means $B_{16}N_{16}H_{32}$ tends to release all hydrogen atoms at lower temperature than $B_{12}N_{12}H_{24}$.

In addition, we have searched the transition structure of the reaction of $B_{16}N_{16} + H_2 \rightarrow B_{16}N_{16}H_2$, and found that the activation barriers of hydrogen adsorption and decompose processes are 33.53 and 42.25 kcal/mol (without ZPE correction), respectively. They are slightly larger than that of the reaction $B_{12}N_{12} + H_2 \rightarrow B_{12}N_{12}H_2$ (31.03 and 40.04 kcal/mol without ZPE correction) [40]. Therefore, both for $B_{12}N_{12}$ and $B_{16}N_{16}$, a proper activator should be considered to reduce their activation barriers, thus they can be used as hydrogen storage nanomaterials.

The main IR active frequency of the N–H and B–H stretching mode of $B_{16}N_{16}H_{32}$ is at 3536 cm^{-1} (T_2 symmetry) and 2498 cm^{-1} (T_2 symmetry), respectively. For $B_{12}N_{12}H_{24}$, the frequency is at 3541 cm^{-1} (T_u symmetry) and 2518 cm^{-1} (T_u symmetry), respectively. They are quite close in the value.

4. Conclusions

In summary, the hydrogenation process of $B_{16}N_{16}$ cage has been studied using ab initio molecular orbital theory with B3LYP/6-31G(d) method and compared with the result of hydrogenation of $B_{12}N_{12}$ cage. The structure characters of the most stable $B_{16}N_{16}H_n$ isomers are discussed in detail. The results show that the average binding energies of hydrogenated $B_{16}N_{16}$ are smaller than that of hydrogenated $B_{12}N_{12}$, especially in high coverage. More delocalized electronic structure is the main reason for why the ABEs of $B_{16}N_{16}H_n$ are smaller than that of $B_{12}N_{12}H_n$. This result also gives a prediction that hydrogenated larger boron nitride cages will have smaller binding energy.

Calculation of the Gibbs free energy of reaction of $B_{16}N_{16} + 16H_2 \rightarrow B_{16}N_{16}H_{32}$ as a function of temperature shows that this reaction will reverse just above about 110 K, which is lower than the reversing temperature 320 K for the reaction of $B_{12}N_{12} + 12H_2 \rightarrow B_{12}N_{12}H_{24}$.

Acknowledgement

This work was supported by the Natural Science Foundations of China (20673070 and 20871077).

Appendix A. Supplementary data

Supplementary data associated with this article can be found, in the online version, at doi:10.1016/j.theochem.2009.11.023.

References

[1] R.D. Cortight, R.R. Davada, J.A. Dumesic, Nature 418 (2002) 964.
[2] J. Alper, Science 299 (2003) 1686.
[3] L. Schlapbach, A. Züttel, Nature 414 (2001) 353.
[4] B. Sakintuna, F.L. Darkrim, M. Hirscher, Int. J. Hydrogen Energy 32 (2007) 1121.
[5] A.W.C. van den Berg, C.O. Arean, Chem. Commun. (2008) 668.
[6] (a) N.L. Roshi, J. Eckert, M. Eddaoudi, D.T. Vodak, J. Kim, M. O'Keeffe, O.M. Yaghi, Science 300 (2003) 1127;
(b) J.L.C. Rowsell, A.R. Millward, K.S. Park, O.M. Yaghi, J. Am. Chem. Soc. 126 (2004) 5666;
(c) X. Lin, J. Jia, P. Hubberstey, M. SchrÖder, N.R. Champness, CrystEngComm 9 (2007) 438.
[7] (a) W. Struzhkin, B. Militzer, W.L. Mao, H.K. Mao, R.J. Hemley, Chem. Rev. 107 (2007) 4133;
(b) M.H.F. Sluiter, H. Adachi, R.V. Belosludov, V.R. Belosludov, Y. Kawazoe, Mater. Trans. 45 (2004) 1452.
[8] R. StrÖbel, J. Garche, P.T. Moseley, L. JÖrissen, G. Wolf, J. Power Sources 159 (2006) 781.
[9] P.O. Krasnov, F. Ding, A.K. Singh, B.I. Yakobson, J. Phys. Chem. C 111 (2007) 17977.
[10] Q. Sun, P. Jena, Q. Wang, M. Marquez, J. Am. Chem. Soc. 128 (2006) 9741.
[11] (a) N.S. Venkataramanan, R. Sahara, H. Mizuseki, Y. Kawazoe, J. Phys. Chem. C 112 (2008) 19676;
(b) H. Woolf, I. Brown, M. Bowden, Curr. Appl. Phys. 8 (2008) 459.
[12] E. Fakioglu, Y. Yurum, T.N. Veziroglu, Int. J. Hydrogen Energy 29 (2004) 1371.
[13] T. Umegaki, J.M. Yan, X.B. Zhang, H. Shioyama, N. Kuriyama, Q. Xu, Int. J. Hydrogen Energy 34 (2009) 2303.
[14] R.T. Paine, C.K. Narula, Chem. Rev. 90 (1990) 73.
[15] T. Oku, T. Hirano, M. Kuno, T. Kusunose, K. Niihare, K. Suganuma, Mater. Sci. Eng. B 74 (2000) 206.
[16] T. Oku, M. Kuno, H. Kitahara, I. Nartia, Int. J. Inorg. Mater. 3 (2001) 597.
[17] G. Mpourmpakis, G.E. Froudakis, Catal. Today 120 (2007) 341.
[18] R.Z. Ma, Y. Bando, H.W. Zhu, T. Sato, C.l. Xu, D.H. Wu, J. Am. Chem. Soc. 124 (2002) 7672.
[19] C.C. Tang, Y. Bando, X.X. Ding, S.R. Qi, D. Golberg, J. Am. Chem. Soc. 124 (2002) 14550.
[20] (a) S.H. Jhi, Phys. Rev. B 74 (2006) 155424;
(b) S.H. Jhi, Y.K. Kwon, Phys. Rev. B 69 (2004) 245407.
[21] (a) E. Durgun, Y.R. Jang, S. Ciraci, Phys. Rev. B 76 (2007) 073413;
(b) N. Koi, T. Oku, Solid State Commun. 131 (2004) 121.
[22] Q. Sun, Q. Wang, P. Jena, Nano Lett. 7 (2005) 1273.
[23] T. Kondo, K. Shindo, Y. Sakurai, J. Alloys Compd. 386 (2005) 202.
[24] Z. Zhou, J.J. Zhao, Z.F. Chen, X.P. Gao, T.Y. Yan, B. Wen, P.R. Schleyer, J. Phys. Chem. B 110 (2006) 13363.
[25] I. Cabria, M.J. López, J.A. Alonso, Nanotechnology 17 (2006) 778.
[26] X.Y. Liu, C.Y. Wang, Y.J. Tang, W.G. Sun, W.D. Wu, J.J. Xu, Physica B 404 (2009) 1892.
[27] T. Teraoa, Y. Bandoa, M. Mitomeb, K. Kurashimab, C.Y. Zhib, C.C. Tangb, D. Golberga, Physica E 40 (2008) 2551.
[28] (a) J. Cheng, R. Ding, Y. Liu, Z.F. Ding, L.B. Zhang, Comp. Mater. Sci. 40 (2007) 341;
(b) S.S. Han, J.K. Kang, H.M. Lee, J. Chem. Phys. 123 (2005) 114703.
[29] (a) X.J. Wu, J.L. Yang, J.G. Hou, Q.S. Zhu, J. Chem. Phys. 121 (2004) 8481;
(b) S.S. Han, S.H. Lee, J.K. Kang, H.M. Lee, Phys. Rev. B 72 (2005) 113402.
[30] T. Oku, M. Kuno, I. Narita, J. Phys. Chem. Solid 65 (2004) 549.
[31] Q. Sun, Q. Wang, P. Jena, Nano Lett. 5 (2005) 1273.
[32] A.Y. Timoshkin, H.F. Schaefer, Inorg. Chem. 44 (2005) 843.

[33] A. SchaumlÖffel, M. Linnolahti, A.J. Karttunen, T.A. Pakkanen, Chem. Phys. Chem. 8 (2006) 62.
[34] H. Wang, H.-S. Wu, J.-F. Jia, Chin. J. Chem. 24 (2006) 731.
[35] A.J. Karttunen, M. Linnolahti, T.A. Pakkanen, J. Phys. Chem. C 112 (2008) 10032.
[36] J.T. Tanskanen, M. Linnolahti, A.J. Karttunen, T.A. Pakkanen, J. Phys. Chem. C 112 (2008) 2418.
[37] G. Seifert, R.W. Fowler, D. Mitchell, D. Porezag, T. Frauenheim, Chem. Phys. Lett. 268 (1997) 352.
[38] (a) D.L. Strout, J. Phys. Chem. A 104 (2000) 3364;
(b) D.L. Strout, J. Phys. Chem. A 105 (2001) 261.
[39] (a) H.-S. Wu, X.Y. Cui, X.F. Qin, D.L. Strout, H.J. Jiao, J. Mol. Model. 12 (2006) 537;
(b) H.-S. Wu, X.Y. Cui, X.F. Qin, H.J. Jiao, J. Mol. Struct. (THEOCHEM) 714 (2005) 153.
[40] J.-F. Jia, H. Wang, X.-Q. Pei, H.-S. Wu, Appl. Surf. Sci. 253 (2007) 4485.
[41] M.J. Frisch et al., Gaussian 03, Revision C.01, Gaussian, Inc., Wallingford, CT, 2004.
[42] H.-S. Wu, X.H. Xu, F.Q. Zhang, H.J. Jiao, J. Phys. Chem. A 107 (2003) 6609.
[43] H. Wang, J.-F. Jia, X.Q. Pei, H.-S. Wu, Chem. Phys. Lett. 423 (2006) 118.
[44] D.L. Strout, Chem. Phys. Lett. 383 (2004) 95.
[45] J.-F. Jia, H.-S. Wu, H.J. Jiao, Acta Chim. Sinica 61 (2003) 653.
[46] X.H. Song, S. Liu, H. Yan, Z.Y. Gan, Physica E 41 (2009) 626.
[47] Y.F. Zhang, Z.F. Liu, J. Phys. Chem. B 108 (2004) 11435.
[48] S. Park, D. Srivastava, K. Cho, Nano Lett. 3 (2003) 1273.
[49] H.-Y. Zhu, T.G. Schmalz, D.J. Klein, Int. J. Quantum Chem. 63 (1997) 393.
[50] (a) B. Mårlid, K. Larsson, J.-O. Carlsson, Phys. Rev. B 60 (1999) 16065;
(b) B. Mårlid, K. Larsson, J.-O. Carlsson, J. Phys. Chem. B 103 (1999) 7637.
[51] J.F. Jia, Y.-N. Lai, H.-S. Wu, H.J. Jiao, J. Phys. Chem. C 113 (2009) 6887.
[52] J.F. Jia, H.-S. Wu, X.-H. Xu, X.-M. Zhang, H.J. Jiao, Org. Lett. 10 (2008) 2573.
[53] L.H. Gan, Chem. Phys. Lett. 421 (2006) 305.
[54] P.F. Weck, E. Kim, S.H. Lepp, N. Balakrishnana, H.R. Sadeghpourc, Phys. Chem. Chem. Phys. 10 (2008) 5184.